Global Increasing Trends in Annual Maximum Daily Precipitation

SETH WESTRA

School of Civil, Environmental and Mining Engineering, University of Adelaide, Adelaide, Australia

LISA V. ALEXANDER

Climate Change Research Centre, Faculty of Science, and Centre of Excellence for Climate System Science, University of New South Wales, Sydney, Australia

FRANCIS W. ZWIERS

Pacific Climate Impacts Consortium, University of Victoria, Victoria, British Columbia, Canada

(Manuscript received 27 July 2012, in final form 6 December 2012)

ABSTRACT

This study investigates the presence of trends in annual maximum daily precipitation time series obtained from a global dataset of 8326 high-quality land-based observing stations with more than 30 years of record over the period from 1900 to 2009. Two complementary statistical techniques were adopted to evaluate the possible nonstationary behavior of these precipitation data. The first was a Mann–Kendall nonparametric trend test, and it was used to evaluate the existence of monotonic trends. The second was a nonstationary generalized extreme value analysis, and it was used to determine the strength of association between the precipitation extremes and globally averaged near-surface temperature. The outcomes are that statistically significant increasing trends can be detected at the global scale, with close to two-thirds of stations showing increases. Furthermore, there is a statistically significant association with globally averaged near-surface temperature, with the median intensity of extreme precipitation changing in proportion with changes in global mean temperature at a rate of between 5.9% and 7.7% K^{-1}, depending on the method of analysis. This ratio was robust irrespective of record length or time period considered and was not strongly biased by the uneven global coverage of precipitation data. Finally, there is a distinct meridional variation, with the greatest sensitivity occurring in the tropics and higher latitudes and the minima around 13°S and 11°N. The greatest uncertainty was near the equator because of the limited number of sufficiently long precipitation records, and there remains an urgent need to improve data collection in this region to better constrain future changes in tropical precipitation.

1. Introduction

Annual maximum daily precipitation data represent one of the most important and readily available measures of extreme rainfall and are used frequently as inputs to assessments of flood risk (Bates et al. 2008; Field et al. 2012; Min et al. 2011). Observational studies of this variable form a critical line of evidence into how precipitation extremes have changed over the instrumental record, and recent findings are showing that at global or continental scales, extreme precipitation events have been increasing in intensity and/or frequency. For example, Alexander et al. (2006) used gridded precipitation data based on 5948 stations globally and found that precipitation changes exhibited a widespread and significant increase. Min et al. (2011), using the same dataset but a different analysis approach, found that 65% of the data-covered areas have positive trends for annual maximum daily precipitation over the period from 1951 to 1999. Groisman et al. (2005) used a different measure of precipitation extremes (the magnitude of the daily precipitation event falling within the top 10% or top 5% of all precipitation events) and found that in the midlatitudes, and in particular over North America, there has been a widespread increase in the frequency

Corresponding author address: Seth Westra, School of Civil, Environmental and Mining Engineering, University of Adelaide, Adelaide, SA 5005, Australia.
E-mail: seth.westra@adelaide.edu.au

DOI: 10.1175/JCLI-D-12-00502.1

of very heavy precipitation events during the past 50–100 years.

These and other studies [e.g., see references in Seneviratne et al. (2012) and Trenberth et al. (2007)], which all differ in their methods of analysis, definition of extreme precipitation indices, and/or the observational datasets used, consistently report increases in extreme precipitation in more land locations globally than locations with decreases. Despite this, there is less confidence in the rate of change and, in particular, how precipitation might scale with atmospheric temperature as the atmosphere warms. Trenberth et al. (2003) provided a physical explanation for why increasing atmospheric temperature might result in an increase in heavy precipitation and suggested that extreme precipitation should scale with the water content of the atmosphere (see also Allen and Ingram 2002). The water content has been found to scale roughly at the Clausius–Clapeyron rate of $\sim 7\%\,K^{-1}$ based on both observational and modeling studies, with the possible exception of the drier land regions, where the scaling appears to be lower (O'Gorman and Muller 2010; Sherwood et al. 2010a; Simmons et al. 2010; Willett et al. 2007). Therefore, based on this hypothesis, one would expect annual maximum daily precipitation to increase in most regions globally at a rate of $\sim 7\%\,K^{-1}$.

Although such theoretical arguments might suggest a relatively uniform sensitivity of extreme precipitation with atmospheric temperature, recent studies on the temperature scaling of extreme precipitation showed that increases above the Clausius–Clapeyron rate are possible, at least for shorter-duration (e.g., hourly) precipitation (Berg et al. 2009; Lenderink and van Meijgaard 2008; Utsumi et al. 2011). Furthermore, several studies examined the temperature scaling of extreme precipitation for a range of durations and exceedance probabilities and found that the rate of change depended on both factors (Hardwick-Jones et al. 2010; Utsumi et al. 2011). Finally, a recent study that looked at the covariation of extreme rainfall and near-surface temperature in Australia also found that the strength of the association with atmospheric temperature depended on the storm burst duration, with daily precipitation scaling rates being significantly below the Clausius–Clapeyron rate of $7\%\,K^{-1}$ (Westra and Sisson 2011). These studies therefore suggest that the scaling of extreme precipitation with temperature may be much more complex than is implied by the Clausius–Clapeyron scaling hypothesis, with various dynamic and thermodynamic factors influencing the relationship between extreme rainfall and atmospheric temperature.

An alternative source of information on the scaling of extreme daily precipitation with atmospheric temperature comes from the outputs of global coupled general circulation models (CGCMs). Numerous CGCM-based studies suggest that the intensity of extreme precipitation will increase under global warming in many parts of the world, including many regions where average precipitation decreases (Kharin and Zwiers 2000, 2005; Semenov and Bengtsson 2002; Voss et al. 2002). A study that evaluated an ensemble of CGCMs participating in the diagnostic exercise for the Intergovernmental Panel on Climate Change (IPCC) for the Fourth Assessment Report found a global multimodel multiscenario sensitivity of about $6\%\,K^{-1}$, although with large intermodel variability (Kharin et al. 2007). That study also examined changes in zonally averaged bands and found much larger increases (but also higher uncertainty) in the tropics compared with other latitudes, and smaller increases in the drier subtropical regions centered on 30°S and 30°N. In an update, Kharin et al. (2013) report that CGCMs participating in phase 5 of the Coupled Model Intercomparison Project (CMIP5) experiment (Taylor et al. 2012) supporting the IPCC Fifth Assessment Report exhibit a planetary multimodel multiscenario sensitivity from 6% to $7\%\,K^{-1}$, but that median local extreme precipitation sensitivity tends to be lower globally ($\sim 5.3\%\,K^{-1}$). Finally, the first formal detection of the observed intensification of extreme precipitation to human-induced increases in greenhouse gases was published by Min et al. (2011), using a comparison of observed and multimodel-simulated changes over the latter half of the twentieth century. This study also noted that models appear to underestimate the sensitivity of annual maximum daily precipitation relative to observations, based on land areas with data coverage, with important implications for how we interpret model-derived projections of future extreme precipitation.

The present observation-based study aims to complement this existing research and focuses on the following three objectives. First, this study updates some of the previous observational studies conducted on annual maximum daily precipitation data using a newly compiled record that represents the most comprehensive, long-running, high-quality record of precipitation extremes currently available. Second, this study examines the relationship between annual maximum precipitation and globally averaged near-surface temperature to determine whether such a relationship exists and the strength of any relationship. Finally, meridional variations in the relationship with near-surface temperature are considered to examine whether there are any large-scale features that might be influencing the observed changes in precipitation extremes.

2. Data

Annual maximum precipitation values were obtained from 11 391 land-based observing stations across the globe. These data represent the most comprehensive, long-running, high-quality data of precipitation extremes currently available and have been used to develop the Hadley Center Global Climate Extremes Index 2 (HadEX2) dataset (Donat et al. 2013). The calculation of these annual precipitation extremes follows the definition of the Rx1day (annual maximum 1-day precipitation amount) index recommended by the joint World Meteorological Organization (WMO) Commission for Climatology (CCl)/Climate Variability and Predictability (CLIVAR)/Joint Technical Commission for Oceanography and Marine Meteorology (JCOMM) Expert Team on Climate Change Detection and Indices (ETCCDI) (Zhang et al. 2011). While there are other datasets that contain more in situ daily precipitation observations, for example, Global Historical Climatology Network (GHCN)-Daily (Durre et al. 2010; Menne et al. 2012), these data are not quality controlled [although quality assurance flags are available for each data point (Durre et al. 2010)] and in many cases contain short or incomplete records (Donat et al. 2013). For example, in the current version of GHCN-Daily, data for India do not generally extend beyond the early 1970s, while in HadEX2 the Rx1day index is available for many stations over the period 1901–2010. However, the number of stations available globally varies greatly over time, reaching a peak in data availability between the 1960s and 1980s (see Fig. 1). In addition, prior to 1950 most of the annual maximum precipitation values are confined predominantly to North America, Europe, India, and Australia. For this study we also removed several stations, mainly over Europe, where it was discovered that the annual maxima did not correspond to any of the available monthly maxima to which we had access. Despite this, the data described in Donat et al. (2013) and used in this study represent the most comprehensive high-quality land-based observations of annual maximum precipitation available.

For this study we use a measure of global near-surface temperature as a covariate for our analysis. Our choice of this covariate is motivated by a number of factors. First, specific humidity globally has risen in concert with a warming atmosphere, and thus, global mean temperature serves as a proxy for the total amount of precipitable water that is available to produce extreme precipitation events (Mears et al. 2007; Sherwood et al. 2010b). Second, in most locations, variations in global mean temperature are positively correlated with those in regional mean temperature (e.g., Mitchell 2003),

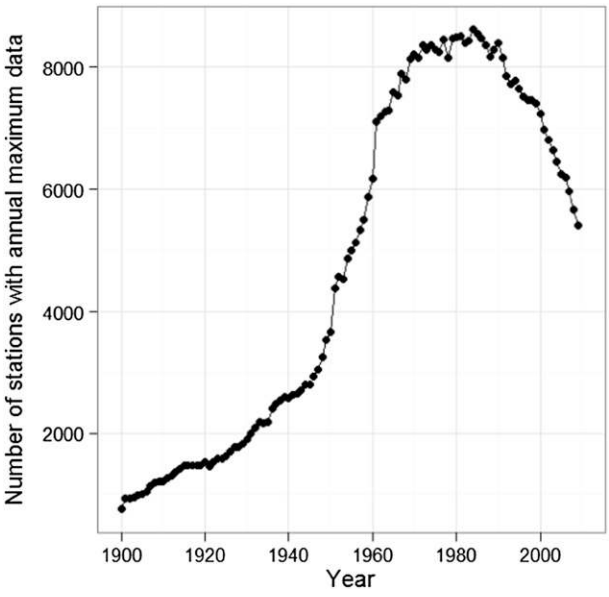

FIG. 1. The total number of stations used in this study that have records in any given year.

which by extension provides information about interannual variations in annual mean precipitable water. In addition, the most reliable attribution of the causes of observed temperature change, and thus the ambient conditions that might affect precipitation extremes, is on the global scale (Hegerl et al. 2007). Many other questions about the dependence of precipitation extremes on temperature could be asked, for example, by considering the local temperatures observed simultaneously with extreme precipitation events. However, the mechanisms that link local contemporaneous temperature variations with precipitation are not necessarily those that link global warming to extreme precipitation change (Trenberth 2011, 2012). First-order local effects tell us little about the quantity of moisture available during extreme events or the relationship between the magnitude of those events and the prevailing thermal state of the region that provided the moisture. Also, the data resources to which we have access do not permit us to perform a detailed analysis of the various aspects of the sensitivity of extreme precipitation to temperature variation on different space and time scales and of the various mechanisms involved. Therefore, we have chosen the global mean near-surface temperature anomaly as a covariate, being broadly representative of internal variations in the thermal state of the climate system.

There are four main independent global near-surface temperature analyses that we could use that extend back to the mid-1800s, and comparisons between all of these globally averaged series show them to be in very good agreement (Kennedy et al. 2010; Sanchez-Lugo et al.

2012). In this case, the National Aeronautics and Space Administration (NASA) Goddard Institute for Space Studies (GISS) series (Hansen et al. 2010) was selected and annual near-surface global temperature anomalies with respect to the 1951–80 base period were used (see Fig. 2). The method for incorporating these two data sources is described in the following section.

3. Methodology

The results in this paper are based on two well-established and complementary statistical methods for testing whether time series data such as annual maximum precipitation are nonstationary. The first method uses the Mann–Kendall nonparametric trend test to evaluate whether there is a monotonic trend in the series. One of the advantages of this test is that it does not make any assumptions on the distribution of the data, other than that under the null hypothesis, the data are independently distributed in time. The second method is based on extreme value theory and tests whether one of the parameters of the generalized extreme value (GEV) distribution, when fitted to the series of annual maximum precipitation, is changing as a function of the global average near-surface temperature anomaly series. This imposes a specific distributional form on the precipitation data (the GEV distribution) that is well supported by statistical extreme value theory, as well as a specific form of the nonstationarity (the global near-surface temperature trend). Finally, it is noted that both methods are univariate and are therefore applied to each station separately. To make inferences about the presence of trends at regional and global scales, a ''field significance'' resampling approach is adopted, accounting for both spatial and temporal dependencies. Each aspect of the statistical methodology is described further below.

a. Mann–Kendall test

The Mann–Kendall test is a widely used nonparametric test for evaluating the presence of monotonic trends in time series data (Chandler and Scott 2011). The test has been applied frequently in analyzing environmental data (Hipel and McLeod 2005), including a number of recent studies that test for changes in rainfall extremes (e.g., Alexander and Arblaster 2009).

We are concerned here with the annual maximum daily rainfall series at a given location. We use the variable m_t, with $t = 1, \ldots, T$, to denote these annual maxima, and with T being the total number of years of data in the record. If we define differences in the data values between different time steps as

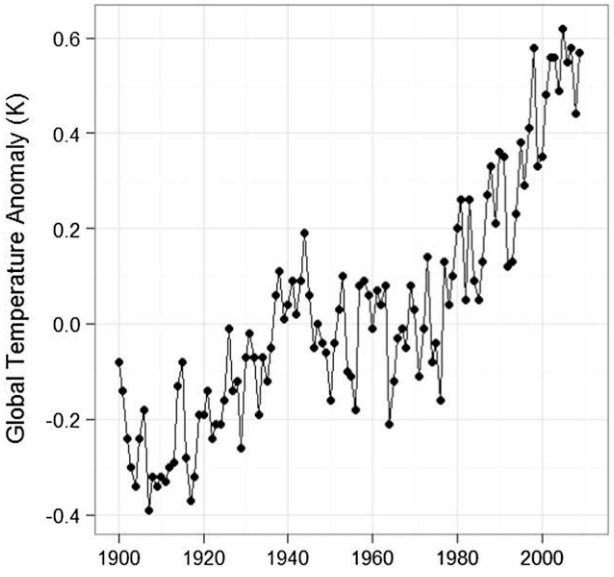

FIG. 2. NASA GISS global near-surface temperature anomaly series in kelvins (Hansen et al. 2010) where anomalies have been calculated with respect to the 1951–80 base period.

$$d(t_1, t_2) = m_{t_2} - m_{t_1}, \tag{1}$$

with $t_2 > t_1$, then the test statistic becomes

$$N = \sum_{t_1=1}^{T-1} \sum_{t_2=t_1+1}^{T} \text{sgn}[d(t_1, t_2)], \tag{2}$$

with $\text{sgn}[d(t_1, t_2)]$ denoting the sign of $d(t_1, t_2)$. The test statistic N represents the number of times m_{t_2} is greater than m_{t_1}, minus the number of times m_{t_1} is greater than m_{t_2}, for all possible combinations of m_{t_2} and m_{t_1} with $t_2 > t_1$. A positive value of N implies that the time series increased more frequently than it decreased (and vice versa for a negative value of N), and the value of N is bounded by $\pm T(T-1)/2$. Kendall's τ is a normalized version of this statistic, which is obtained by dividing by this upper bound

$$\tau = \frac{2N}{T(T-1)}, \tag{3}$$

so that τ is bounded by $[-1, 1]$. Assuming the data are serially independent, the null hypothesis can be approximated by a normal distribution, with more details in Chandler and Scott (2011). The median value of the autocorrelation coefficient of the annual maximum precipitation across all global stations with more than 30 years of record was found to be 0.0017; therefore, the assumption of serial independence appears to be valid on average. The Mann–Kendall analysis was conducted using the R package ''Kendall'' (McLeod 2011).

b. The nonstationary generalized extreme value model

The statistical characteristics of very small and large values of a distribution has been an area of active research over the past few decades and has led to the emergence of extreme value theory as the unifying theory describing the statistical behavior of such extremes (Gumbel 1958; Leadbetter et al. 1983). One of the most commonly studied instances of an extreme concerns the maximum of a stationary time series that satisfies appropriate mixing conditions (e.g., Leadbetter et al. 1983), $X_1, \ldots, X_n$, written as

$$M_n = \max\{X_1, \ldots, X_n\}, \tag{4}$$

where we use the uppercase M to denote a random variable representing the maximum value over a block of n observations (e.g., see Coles 2001). In our application, X represents a time series of daily total rainfall at a given site, and n is a block size of 365 days (or 366 days for leap years), such that M_n denotes the annual maximum rainfall in a given year.

It can be shown that under fairly general conditions, the probability distribution of a normalized version of M_n converges in distribution to one of three families of extreme value distributions, denoted by $G(z)$ (Fisher and Tippett 1928; Gnedenko 1943; Jenkinson 1955; von Mises 1954) as $n \to \infty$. These families are known as the Gumbel, Fréchet, and Weibull distributions and can be combined into a single distribution known as the GEV distribution:

$$G(z) = \exp\left\{-\left[1 + \xi\left(\frac{z-\mu}{\sigma}\right)\right]^{1/\xi}\right\}, \tag{5}$$

where $\mu, \sigma > 0$, and ξ are the location, scale, and shape parameters, respectively. Although the theory applies in the general case only in the limit as $n \to \infty$, in practice this result allows the GEV distribution to be substituted as an approximation to the actual distribution of observed block maxima for finite n, and there is now substantial literature on the use of this distribution for both observed and climate model–simulated annual maximum precipitation series (e.g., Coles et al. 2003; Kharin and Zwiers 2005; Kharin et al. 2007; Min et al. 2009; Westra and Sisson 2011).

We are interested here in how the behavior of random variable Z changes over time and, in particular, whether the observations of the annual maximum daily rainfall accumulation can be represented as random year-to-year fluctuations from a stationary probability distribution (the null hypothesis) or whether the distribution is changing systematically through time. Written more precisely, we are interested in testing the hypothesis that one of the parameters of the GEV distribution, the location parameter, is changing through time:

$$Z_t \sim \mathrm{GEV}[\mu(t), \sigma, \xi], \tag{6}$$

with

$$\mu(t) = \beta_0 + \beta_1 y(t) \tag{7}$$

and with $y(t)$ denoting a time-varying covariate and β_0, β_1 representing unknown parameters to be estimated. In our analysis, $y(t)$ is the global average near-surface temperature in year t. We also modeled a time-varying scale parameter $\sigma(t)$ [see, e.g., Kharin and Zwiers (2005)] to each of the gauges and found the results were very similar to the results when only modeling a nonstationary location parameter. Therefore, the results presented in this paper are based on the more parsimonious location-only model.

We use the method of maximum likelihood to estimate all the model parameters, and we adopt a likelihood ratio test for the hypothesis testing. The test is able to handle missing years of record since only those years with data are included in the likelihood function, and therefore an uninterrupted rainfall record is not required. We only impose a constraint that the record length must be above some minimum number of years, with various thresholds adopted in the analysis as described in more detail in section 4. Further details on the methodology are available in Coles (2001). The extreme value analysis was conducted using the R package ''evd'' (Stephenson 2002).

c. Calculating field significance

Although standard inferential techniques exist for evaluating univariate tests such as those described above, application to spatial datasets where there is spatial dependence is much more complex. For example, in the case of extreme value distributions, spatial analogs of the univariate extreme value distribution have only recently been developed (Padoan et al. 2010), and limited research has been conducted on using such techniques for modeling the nonstationarity of climate data such as precipitation (Westra and Sisson 2011). Furthermore, these applications focused on subcontinental-scale spatial rainfall using only 46 and 35 stations for the Padoan et al. (2010) and Westra and Sisson (2011) studies, respectively. At present, the application of such techniques to large amounts of global data is computationally infeasible.

As an alternative, for the present study we use a field significance resampling-based procedure (von Storch and Zwiers 1999; Wilks 2011) where we calculate the test statistics on the observed time series, as well as 1000

resampled replicates, to evaluate the probability that the test statistics are significant under the null hypothesis and that the annual maximum data are stationary. A range of test statistics were considered, including the percentage of locations with statistically significant covariance with temperature for the nonstationary GEV analysis and the percentage of locations with statistically significant trends for the Mann–Kendall test. To ensure that spatial dependence is maintained, we form matrix $\mathbf{m}$, which is a $T \times S$ matrix in which the rows T denote time and the columns S denote the spatial location. Then each resampled matrix involves drawing (with replacement) T rows from $\mathbf{m}$ to form $\mathbf{m}^*$, thereby ensuring the sequencing of the series in time is lost but the dependencies across space are preserved. This enables us to test whether the annual maximum data globally or over specific geographic domains are nonstationary.

Finally, although in section 3a it was indicated that the autocorrelation of m_t was close to zero on average across all stations globally, we evaluated the need for using a moving blocks bootstrap that accounts for autocorrelation. This approach is described in Wilks (1997) and is based on calculating a variance inflation factor that uses the autocorrelation at all lags to estimate the time between ''effectively independent samples.'' Other studies that have investigated either observed or modeled trends in precipitation extremes have used such a block bootstrapping approach, finding that a block size of two or three was usually required to account for autocorrelation effects (e.g., Alexander et al. 2006; Kiktev et al. 2003, 2007). These studies were based on the characteristics of precipitation data with longer aggregation periods, and by contrast, the outcome of our analysis using the annual maximum data was that using a block size greater than one was not necessary. We therefore adopted only the conventional spatial bootstrap procedure for most of the analyses.

4. Results

a. Mann–Kendall test

We commence by examining the presence of monotonic trends in the Rx1day data using the Mann–Kendall test. As discussed in the previous section, this test does not make distributional assumptions on the data, nor does it impose a specific form on the trend other than that it increases or decreases monotonically. The assumption that the data are serially independent was discussed in section 3a, and no evidence for significant autocorrelation was found.

We conduct our analysis on all stations with more than 30 years of data over the period from 1900 to 2009. These criteria were selected to maximize the number of stations available for inference, while at the same time excluding very short records. A total of 8326 out of the 11 391 records met these criteria, and the median length of record for stations meeting these criteria was 53 years. On the basis of the test statistic described in section 3a, we classified each station as ''significant increasing,'' ''significant decreasing,'' and ''no significant'' trend, using a 5% two-sided significance level. This significance level implies that about 2.5% of stations would show significant increasing and significant decreasing trends by random chance.

The results showed that 8.6% of stations had significant increasing trends, while 2.0% had significant decreasing trends. To test whether this is statistically different from the null hypothesis that there are no trends, we use the resampling methodology described in section 3c to generate a distribution of the percentage significant increasing and decreasing trends under the null hypothesis that there are no trends. The results of this analysis are shown in Fig. 3, and the observed percentage of stations with significant increasing trends clearly falls outside this distribution. In contrast, the observed percentage of stations with significant decreasing trends falls within the null hypothesis distribution. We note that, although the discussion in section 3c showed that moving block bootstrapping was not required, we repeated the analysis using a block size of 4 years [well above the value of 2 or 3 recommended in Kiktev et al. (2003)], and the results were consistent with our original analysis.

Another way of presenting the results involves examining the percentage of stations showing increasing and decreasing trends and evaluating the probability that this is occurring under the null hypothesis that there is no significant trend. On the basis of the observed precipitation data, we find that 64% of stations show increasing trends and 36% show decreasing trends. This is close to the finding by Min et al. (2011) that 65% of grid boxes had positive trends, using 1-day annual maximum data from the HadEX gridded extremes dataset over the period from 1951 to 1999. We evaluated the distribution of increasing and decreasing trends under the null hypothesis, and the distribution is shown in Fig. 4. As expected, on average, about 50% of stations show increases and 50% show decreases under the null hypothesis, and the observed percentage of stations showing increases falls clearly outside of this distribution.

b. Nonstationary generalized extreme value analysis

In the previous section we established that there is a significant increasing trend in annual maximum precipitation on average at the global scale. We now examine

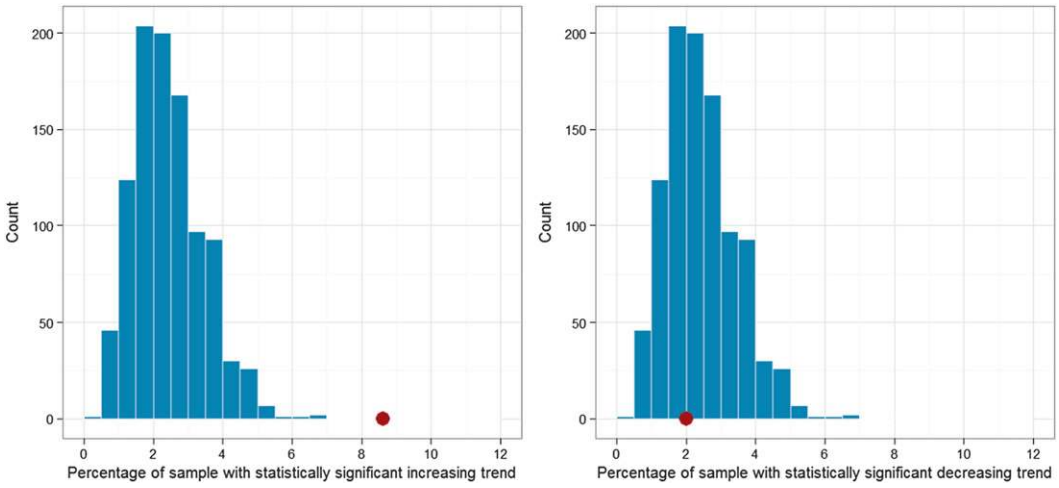

FIG. 3. Percentage of stations showing statistically significant (left) increasing and (right) decreasing trends based on the Mann–Kendall test. The histogram represents the distribution of results from 1000 bootstrap realizations of the global annual maximum rainfall data, and the red dot represents the value from the observed data.

this issue in more detail by conducting a nonstationary extreme value analysis using the global near-surface temperature trend as the covariate. Similar to the Mann–Kendall test described above, we commence by analyzing the set of 8326 stations with more than 30 years of data over the period from 1900 to 2009, with the average record length being 53 years. We also analyze longer periods of record and different time windows and discuss the results from these alternative analyses later in this section.

We use the likelihood ratio test to evaluate the hypothesis that the extremes are varying in response to global mean near-surface temperature variations against the null hypothesis that there is no significant covariation. To this end, we classified stations as ''significant positive association,'' ''significant negative association,'' and ''no significant association'' with the global mean near-surface temperature series. Once again, we used a 5% significance level, which means that under the null hypothesis, about 2.5% of stations should show significant positive association and about 2.5% should show significant negative association by random chance.

1) GEOGRAPHIC DISTRIBUTION OF STATIONS EXHIBITING SIGNIFICANT TRENDS

The results of the analysis show that 10.0% of stations globally had statistically significant positive associations with the annual global mean near-surface temperature series and 2.2% had significant negative associations. The spatial locations of these stations are given in Fig. 5, and the larger number of positive associations relative to negative associations is clearly apparent. The uneven geographic distribution of stations is also evident, with locations that have long records being well represented in North America (particularly the United States), western Europe, and South Africa. In contrast, the majority of the African landmass, Indonesia, parts of South America, and the sparsely populated areas of Australia are particularly poorly represented, either because the records are unavailable or because they were shorter than the 30-yr threshold used in this analysis.

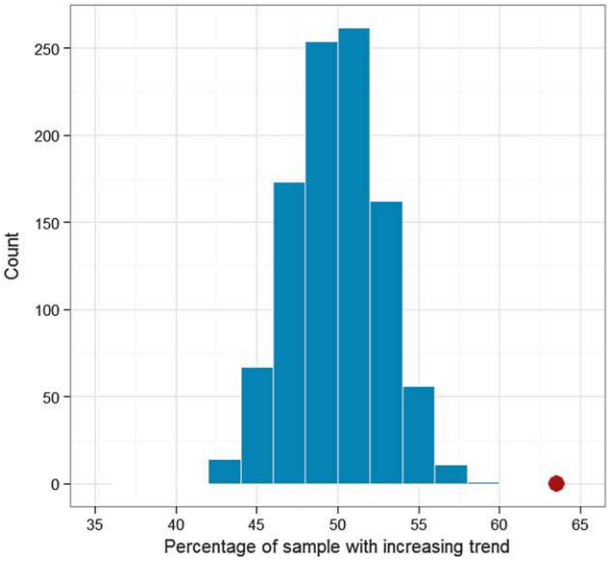

FIG. 4. Percentage of sample with increasing trends based on the Mann–Kendall test. The blue histogram was obtained from resampling with 1000 replicates, and the red dot was based on the observed sample.

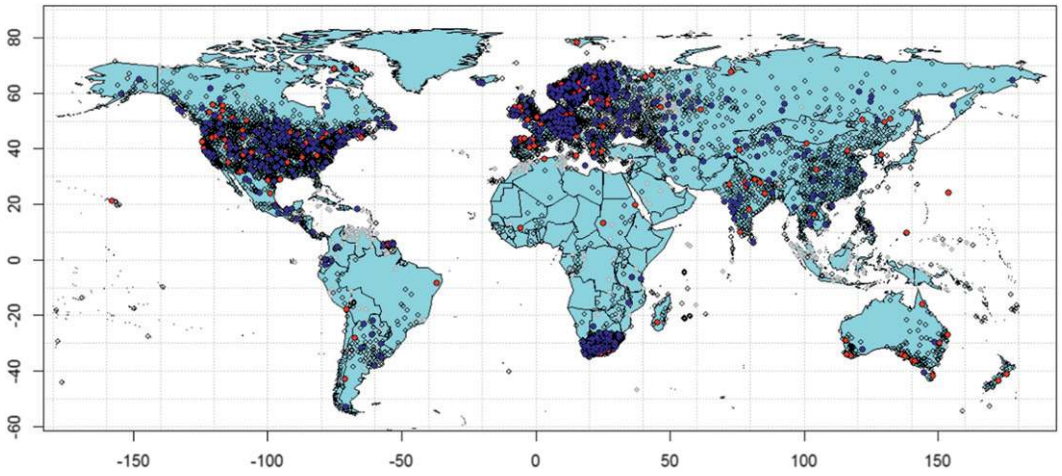

FIG. 5. Plot of the outcome of the nonstationary generalized extreme value analysis for each of 8326 stations that met specified selection criteria (see text). Solid blue (red) dots indicate a statistically significant positive (negative) relationship with the global mean near-surface temperature anomaly series at the 5% (two sided) significance level, while open black dots indicate no statistically significant relationship. Solid gray dots indicate that the series was too short for inclusion in the analysis.

Another feature of this plot is that, although the number of stations with increasing trends outnumber the stations with decreasing trends, it is difficult to isolate a clear geographic pattern associated with the increases [see also Min et al. (2011)]. For example, visually inspecting the landmass covered by Russia, Mongolia, China, and India, the stations with increases and decreases appear to be randomly distributed over the domain. Similar conclusions appear to hold for South America and Australia, except in the latter case, where there are a larger number of stations with decreasing trends relative to stations with increasing trends. These results are consistent with what is expected under an enhanced greenhouse gas climate, with Kharin et al. (2007) anticipating an intensification of precipitation extremes in most regions, except in areas of downwelling atmospheric circulation in the subtropics.

Examining the magnified plot of North America (Fig. 6), it is again difficult to discern visually any clear spatial pattern. Similar results are also apparent for Europe (Fig. 7), although for this continent a larger degree of spatial clustering can be observed that might be related to the high station density in this region. This is particularly evident for the region around the Netherlands, Belgium, western Germany, and southern Scandinavia, where the gauging density is highest. Finally, the magnified plot of southern Africa (Fig. 8) shows that the stations with significant decreases only occur in the eastern half of the country, although based on visual inspection, it is difficult to infer whether this pattern is from sampling variability or a coherent signal.

2) A SIGNIFICANT RELATIONSHIP WITH GLOBAL MEAN NEAR-SURFACE TEMPERATURE?

It was discussed in the previous section that of all the stations analyzed, more than 4 times the number of stations showed significant positive associations with global mean near-surface temperature anomalies compared with significant negative associations. Can this result be attributed to random variability under the null hypothesis that the extremes from one year to the next are independently distributed, or does this result indicate there may be a significant positive association with global temperature in the data?

We resample the global precipitation data 1000 times to generate a distribution of the fraction of stations showing statistically significant positive and negative

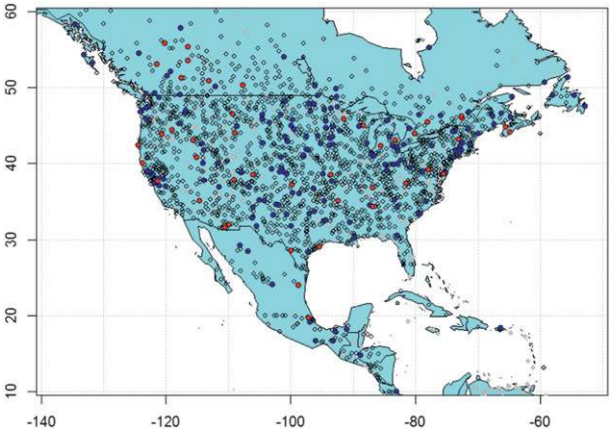

FIG. 6. As in Fig. 5, but for North America.

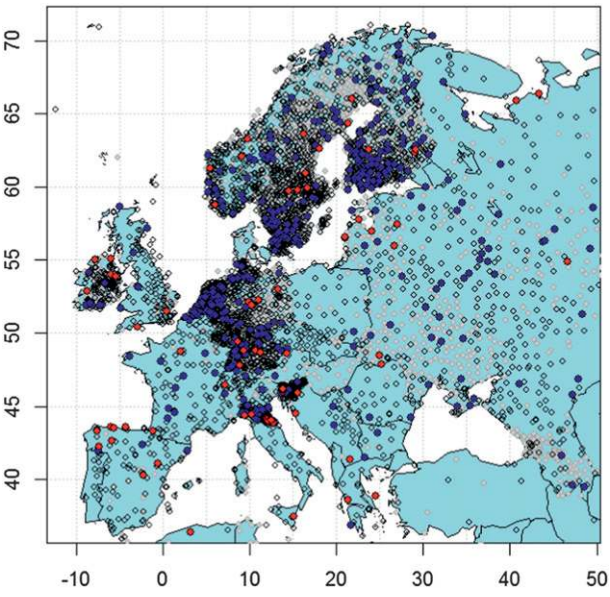

FIG. 7. As in Fig. 5, but for Europe. For visualization purposes, red dots overlay blue dots.

associations and compare this with the fraction of stations showing significant positive and negative associations in the original data. The results are shown in Fig. 9. In the case of positive associations (left panel), it is clear that the observed value of 10.0% is substantially outside the distribution obtained from the resampled data, indicating that the observations do not appear to be consistent with the null hypothesis. In fact, not a single sample out of the 1000 realizations showed a percentage of stations with significant positive associations that are similar to the value observed. In contrast, considering the distribution of negative associations (right panel), the observed value of 2.2% falls comfortably inside the distribution of negative associations obtained by resampling.

A different way of expressing these results is provided in Fig. 10. Here, we estimate the percentage increase in annual maximum daily precipitation per kelvin of global surface temperature change, which can be evaluated directly once the model in Eq. (6) has been fitted to the data. The percentage change per kelvin was estimated at all stations, and the distribution of percentage increases is shown, along with whether the association between annual precipitation extremes and the global mean temperature anomalies is significant or not. The distribution of the percentage of stations with positive associations with temperature shows that a greater number of stations have estimated positive associations (65%) relative to negative associations (35%). As the absolute magnitude of the percentage change per kelvin increases, the proportion of stations with statistically

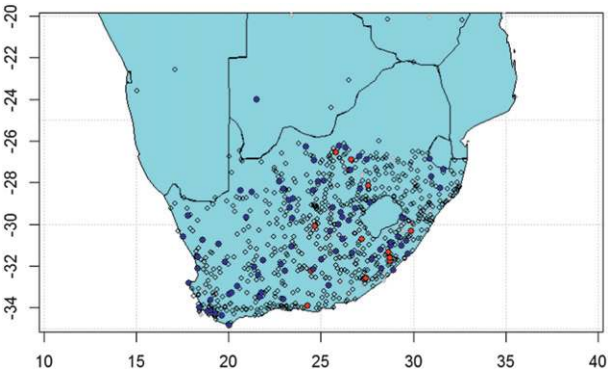

FIG. 8. As in Fig. 5, but for southern Africa.

significant changes also increases, although large percentage changes that are not statistically significant can also be observed. This is because the length of record for each station is different, and the magnitude of variability relative to the underlying trend (the signal-to-noise ratio) therefore also varies from one station to the next, and the inference takes this into account.

Considering all stations—both significant and not significant—together, the median percentage increase in annual maximum precipitation per kelvin of global surface temperature increase was found to be 7.7%. Once again, it is possible to use a resampling technique to evaluate the significance of this result, and it can be seen (Fig. 11) when comparing this value with the distribution of resampled data that the magnitude of the global average extreme precipitation sensitivity was significantly different to the range that could be expected under the null hypothesis.

3) LATITUDINAL VARIATION OF TRENDS

The latitudinal variations of the trends are now investigated to determine whether the finding of a median sensitivity of 7.7% K^{-1} globally is distributed evenly or whether there are distinct meridional features. To this end, we look at the fraction of stations exhibiting statistically significant associations with global near-surface temperature, as well as the median value of the change per kelvin of temperature, within a $\pm 5°$ latitudinal moving window. This is repeated for the resampled data to obtain confidence intervals for each latitudinal band.

Before interpreting the results, it is important to note the uneven distribution of observing stations in the different latitudinal bands. This is shown in the top panel of Fig. 12, which depicts the number of stations that meet the minimum criterion of a 30-yr record length. The results show a maximum around 48°N latitude (representing a band from 43° to 53°N latitude), encompassing the northern half of the United States and southern

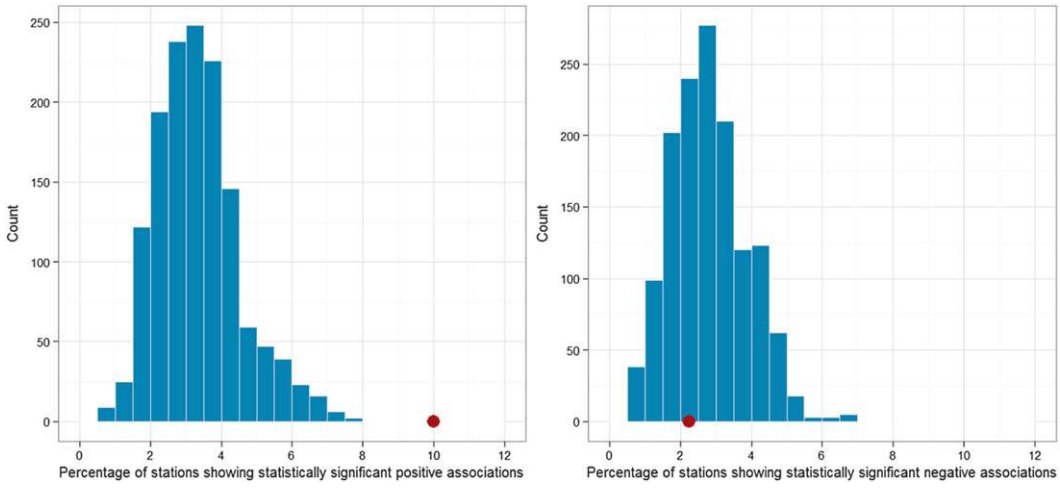

FIG. 9. Fraction of stations showing statistically significant (left) positive and (right) negative association between variations in extreme precipitation and global mean near-surface temperature anomalies. The histogram represents the distribution of results from 1000 bootstrap realizations of the global annual maximum rainfall data, and the red dot represents the value from the observed data.

Canada, together with a large portion of Europe and Russia. A second maximum is in the Southern Hemisphere around 30°S (25°–35°S) latitude and encompasses the densely gauged portions of Brazil, South Africa, and Australia. In between these two latitude bands is a minimum value near the equator, with the lowest value of only 59 stations in the band centered on 1°N latitude. This is almost two orders of magnitude less than the Northern Hemisphere maximum value, highlighting the importance of improved monitoring and coordinated data collection efforts at equatorial latitudes. Finally, an examination of the station locations in Fig. 5 shows that the data is not evenly distributed zonally, partly because of the uneven sampling distribution of the precipitation

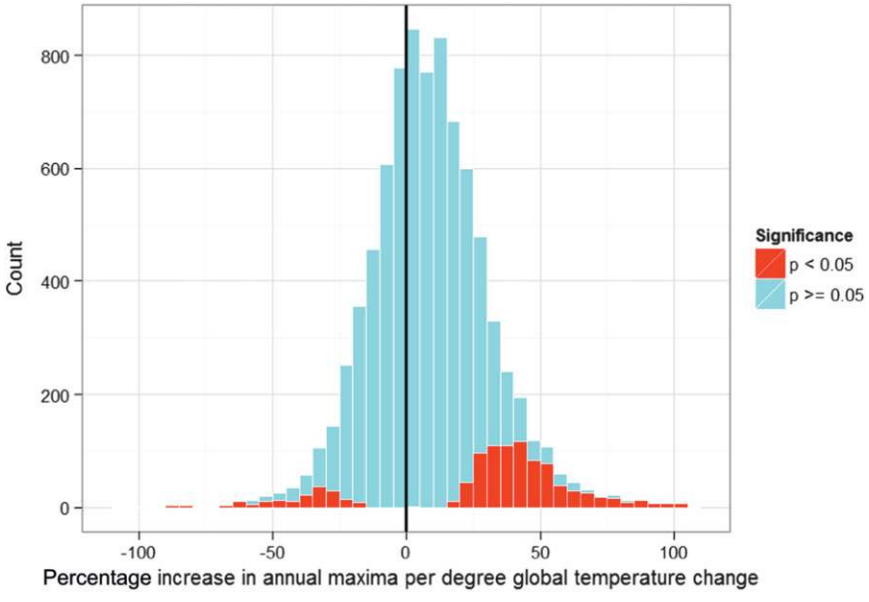

FIG. 10. Histogram of percentage increase in annual maximum rainfall per kelvin global average surface temperature change for each of the 8326 stations that met specified selection criteria (see text). Red coloring indicates the relationship is statistically significant at the 5% level.

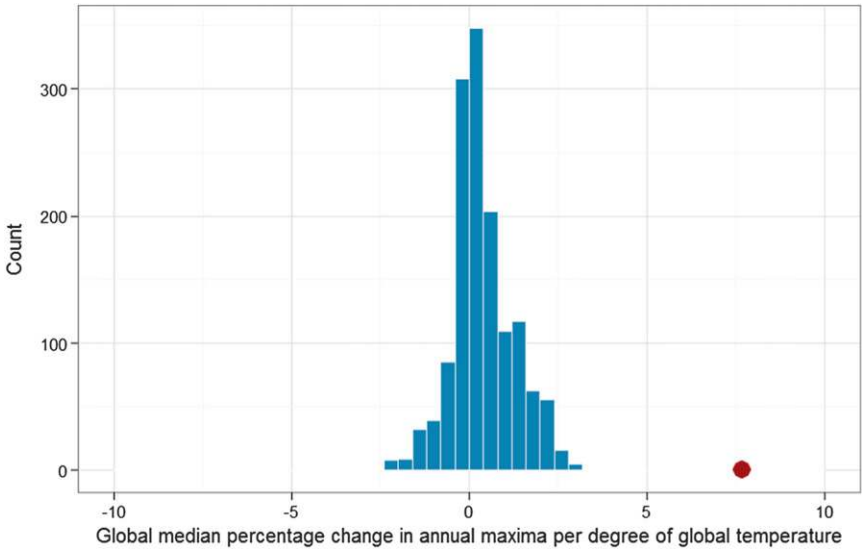

FIG. 11. Global median of estimates of the local sensitivity of annual precipitation extremes to a 1-K increase in global mean near-surface temperature. The histogram represents the distribution of results from 1000 bootstrap realizations of the global annual maximum rainfall data, and the red dot represents the value from the observed data.

gauges and partly because of the uneven distribution of land areas and oceans; this should also be taken into account when interpreting the results.

Considering first the fraction of stations exhibiting significant increases (Fig. 12, middle), it can be seen that there are some clear meridional variations, with the largest proportion of stations that have positive association with global mean near-surface temperature located near the equator and a second maxima at about 55°N. The two locations with the minimum fraction of significant positive associations are at 15°S and 6°N. It is noted that the resampling methodology takes the lower sample sizes near the equator into account, with the confidence interval being much wider in the less well gauged parts of the domain. The results of our analysis are reasonably consistent with the model-derived results under a future greenhouse gas–enhanced climate (Kharin et al. 2007), except that the latitudes with the minimum fraction of positive associations are closer to the equator compared with the modeling studies.

Finally, we plot the median estimate of the sensitivity of annual extreme precipitation per kelvin warming by latitude (Fig. 12, bottom). The general pattern reflects the conclusions of the middle panel, with the largest positive associations near the equator and a second maxima occurring in the higher latitudes of the Northern Hemisphere. Minima exist at 13°S and 11°N, and both these minima are not statistically significantly different from the null hypothesis, which is that there is no trend at these latitudes.

4) IMPLICATIONS WHEN USING DIFFERENT DATA PERIODS

All of the results from the preceding analysis were based on the set of stations between 1900 and 2009 with at least 30 years of data, with the median number of years per station in this dataset being 53 years. As discussed in section 2, the number of stations with rainfall data increased significantly in the first half of the twentieth century, plateauing from about 1960. Therefore, the majority of the dataset is likely to be from the latter part of the record, although sequences from the early part of the twentieth century are also included in the analysis.

To ensure that the results are not substantially influenced by the period of record or the median length of record, we conduct the analysis on different subsets of data, summarized in Table 1. The first three analyses consider the full period from 1900 to 2009 but use different thresholds for the minimum record length. The last two analyses are for the different periods of record, with the first 60 years of the twentieth century compared with the last 40 years of the twentieth century and the first 10 years of the twenty-first century.

Considering the first three analyses, it can be seen in Table 1 that by increasing the minimum number of years to be analyzed from 30 to 70 years, the number of stations meeting this minimum threshold drops dramatically from 8326 stations to 2124 stations. Interestingly, the percentage of stations with positive associations, and

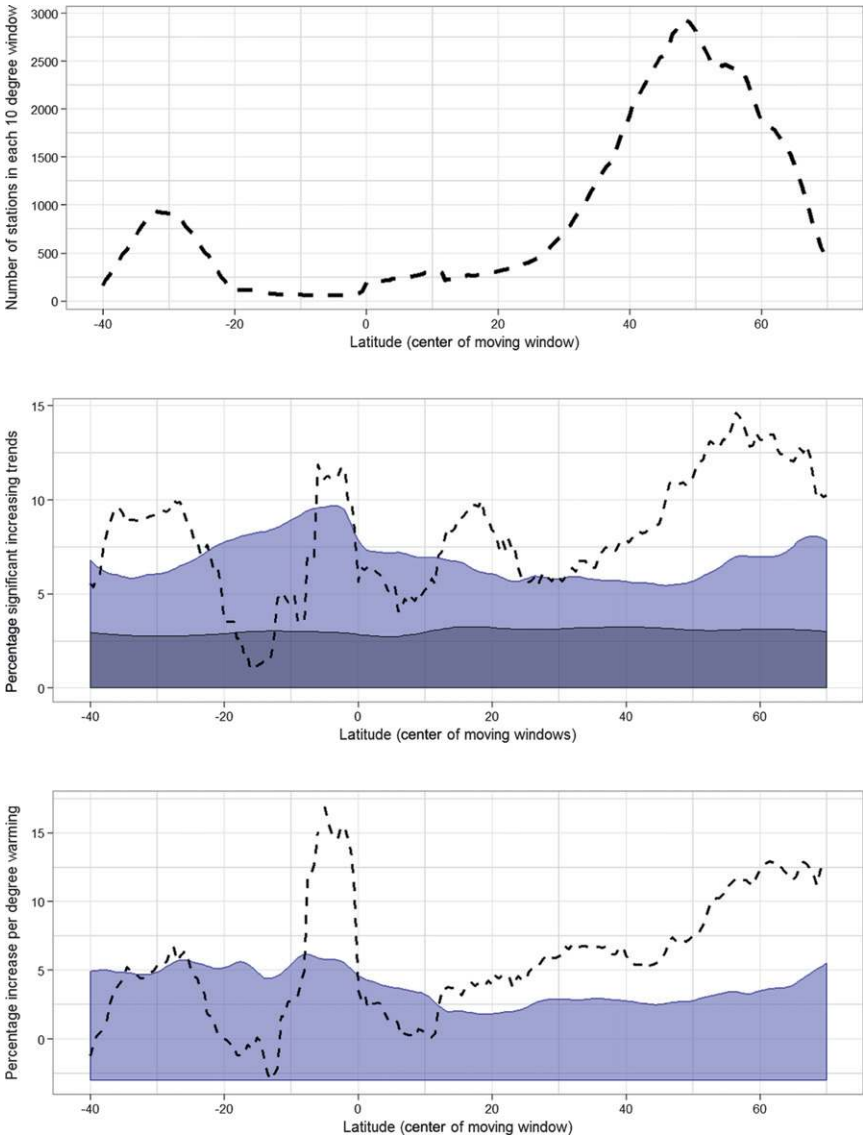

FIG. 12. Variation in the estimated sensitivity of annual maximum precipitation to a 1 K increase in global mean temperature by latitude. (top) The number of stations within each ±5° latitude band. (middle) The fraction of stations exhibiting significant positive association, with light blue shading indicating the upper 97.5% confidence bound and dark blue shading indicating the median of the confidence interval. (bottom) Sensitivity (%) of annual maximum precipitation per kelvin warming of global near-surface temperature, with light blue shading indicating the upper 97.5% confidence bound.

the median sensitivity, is remarkably constant (ranging from 6.5% K^{-1} for the longest threshold to 7.7% K^{-1} for the shortest threshold), indicating an absence of systematic biases caused by record length. The percentage of stations with significant positive associations increases from 10.0% (30-yr threshold) to 11.7% (70-yr threshold). This is likely to be because of the enhanced statistical power of the likelihood ratio test for longer records.

Considering the two subperiods, it can be seen that results are again very consistent with those of the preceding analysis. For the period from 1900 to 1959, on average, 59% of stations show positive association, with a median percentage increase of 5.9% K^{-1} global average surface temperature. The more recent period from 1960 to 2009 shows a slightly higher percentage of stations with increasing trends and a temperature sensitivity of 7.2% K^{-1}. The general conclusion appears to be that neither record length nor sampling period has a substantial effect on the relationship between annual maximum precipitation and globally averaged near-surface temperature.

TABLE 1. Percentage of stations with significant associations between annual precipitation extremes and global mean temperature anomalies and the estimated median sensitivity of annual extreme precipitation per kelvin of warming in global mean surface temperature for the various time periods shown. In columns 7 and 8, negative values are indicated with parentheses.

Test	Refer to section	Period	Min record length (yr)	Median record length (yr)	No. stations meeting criteria	Stations with + (−) associations (%)	Stations with significant + (−) associations (2.5% significance level) (%)	Median sensitivity (%) for a 1-K increase in global mean near-surface temperature
Mann–Kendall trend test	4a	1900–2009	30	53	8326	64 (36)	8.6 (2.0)	—
Likelihood ratio test of nonstationary GEV*	4b(1)	1900–2009	30	53	8326	65 (35)	10.0 (2.2)	7.7
	4b(4)	1900–2009	50	65	4839	66 (34)	10.4 (2.3)	6.9
	4b(4)	1900–2009	70	88	2124	65 (35)	11.7 (2.9)	6.5
	4b(4)	1900–59	30	48	1947	59 (41)	5.8 (3.0)	5.9
	4b(4)	1960–2009	30	45	7675	64 (36)	8.8 (2.4)	7.2
Likelihood ratio test of nonstationary GEV**	4b(5)	1900–2009	30	53	8326	—	—	7.0

* Nonstationary location parameter only.
** Weighted median sensitivity taking into account different geographic densities of gauges.

5) IMPLICATIONS OF UNEVEN GEOGRAPHIC COVERAGE

To account for the uneven geographic distribution of stations, a revised estimate of the sensitivity of annual maximum precipitation to global mean near-surface temperature was calculated. The approach adopted was to 1) divide the world into 1° latitude × 1° longitude grid boxes, 2) calculate the mean sensitivity across all of the stations within each grid box, and 3) construct an area-weighted global average sensitivity from the gridbox averages. This weighted average significantly reduces the importance attached to stations in highly gauged regions (e.g., in parts of Europe) relative to other less densely gauged parts of the world and is therefore expected to provide an estimate of the sensitivity of global land annual maximum precipitation with globally averaged near-surface temperature that is more representative of a typical location with observations.

These results are also shown in Table 1 and demonstrate that median global land sensitivity is 7.0% K^{-1} change in global near-surface temperature. This is consistent with the unweighted results and therefore suggests that the uneven geographical coverage does not have a large bearing on the estimated global temperature sensitivity of annual maximum precipitation.

5. Discussion and conclusions

In this study a large, high-quality dataset of annual maximum daily precipitation has been analyzed to evaluate the presence of trends at global and regional scales. The analysis was based on the application of two complementary statistical methods: one that tested for monotonic trends and the other that tested for a significant association with globally averaged near-surface atmospheric temperature. Consistent with the findings of Min et al. (2011), the results showed that nearly two-thirds of rainfall stations globally exhibited increasing trends, with these increases being statistically significantly different from the null hypothesis, which is that there is no global trend. Furthermore, the nonstationary extreme value analysis showed a statistically significant positive association with near-surface atmospheric temperature, with a global median value ranging from 5.9% to 7.7% K^{-1}, depending on the method of analysis used.

The consistency of the results between the Mann–Kendall and nonstationary generalized extreme value analysis is remarkable, as is the consistency of the results when using different observational periods. In particular, a median sensitivity in annual maximum precipitation data with a 5.9% intensification of annual precipitation extremes per kelvin of warming globally was found when

only considering records longer than 30 years over the period from 1900 to 1959, and a median sensitivity of 7.2% K^{-1} was found when considering records from 1960 to 2009, which suggested a relatively stable association with globally averaged near-surface temperature. Whether such an association will continue into the future as the atmosphere warms is an important research question, and the study by Kharin et al. (2007) found a model-averaged increase of 6% K^{-1}, with most models having sensitivities in the range of 4%–10% K^{-1} when considering the 20-yr return values of annual extremes of 24-h precipitation amounts. A recent update based on the CMIP5 experiment (Kharin et al. 2013) draws similar conclusions.

The meridional variation in the magnitude of the association with temperature was also interesting, with the greatest positive associations occurring in the tropics in a band roughly between 6°S and 3°N, and minima at both 13°S and 11°N. The higher latitudes also showed stronger positive associations, particularly in the Northern Hemisphere above about 50°N. We note, however, the uneven distribution of stations across the globe, with some regions much better represented than others. The tropics are particularly poorly sampled, and the strong positive association between annual maximum precipitation and global near-surface temperature highlights the importance of improved monitoring in these latitudes.

Finally, we emphasize that caution is required in interpreting our finding of a median rate of change of annual maximum daily precipitation of 7% K^{-1} global mean near-surface temperature. This rate is similar to that implied by the Clausius–Clapeyron relationship, which would suggest that precipitation extremes are increasing in accord with the increase in atmospheric moisture. However, our results show distinct meridional variations, highlighting that other factors such as changes in atmospheric circulation may also be important in explaining the observed changes. Furthermore, as highlighted in the introduction, these results only apply to daily time scale precipitation extremes and cannot necessarily be applied to shorter-duration time scales.

Acknowledgments. Westra was supported by Australian Research Council Grant DP120100338. Alexander and Zwiers are supported by Australian Research Council Grant LP100200690. Zwiers was also supported by the Canadian Foundation for Climate and Atmospheric Sciences.

REFERENCES

Alexander, L. V., and J. M. Arblaster, 2009: Assessing trends in observed and modelled climate extremes over Australia in relation to future projections. *Int. J. Climatol.,* **29,** 417–435.

——, and Coauthors, 2006: Global observed changes in daily climatic extremes of temperature and precipitation. *J. Geophys. Res.,* **111,** D05101, doi:10.1029/2005JD006290.

Allen, M. R., and W. J. Ingram, 2002: Constraints on future changes in climate and the hydrological cycle. *Nature,* **419,** 224–232.

Bates, B. C., Z. W. Kundzewicz, S. Wu, and J. P. Palutikof, Eds., 2008: Climate change and water. IPCC Tech. Paper 6, 210 pp. [Available online at http://www.ipcc.ch/pdf/technical-papers/climate-change-water-en.pdf.]

Berg, P., J. O. Haerter, P. Thejll, C. Piani, S. Hagemann, and J. H. Christensen, 2009: Seasonal characteristics of the relationship between daily precipitation intensity and surface temperature. *J. Geophys. Res.,* **114,** D18102, doi:10.1029/2009JD012008.

Chandler, R. E., and E. M. Scott, 2011: *Statistical Methods for Trend Detection and Analysis in the Environmental Sciences.* John Wiley & Sons, 368 pp.

Coles, S. G., 2001: *An Introduction to Statistical Modelling of Extreme Values,* Springer, 208 pp.

——, L. R. Pericchi, and S. A. Sisson, 2003: A fully probabilistic approach to extreme value modelling. *J. Hydrol.,* **273,** 35–50.

Donat, M. G., and Coauthors, 2013: Updated analysis of temperature and precipitation extreme indices since the beginning of the twentieth century: The HadEX2 dataset. *J. Geophys. Res.,* **118,** 2098–2118, doi:10.1002/jgrd.50150.

Durre, I., M. J. Menne, B. E. Gleason, T. G. Houston, and R. S. Vose, 2010: Comprehensive automated quality assurance of daily surface observations. *J. Appl. Meteor. Climatol.,* **49,** 1615–1633.

Field, C. B., and Coauthors, 2012: *Managing the Risks of Extreme Events and Disasters to Advance Climate Change Adaptation.* Cambridge University Press, 582 pp.

Fisher, R. A., and L. H. C. Tippett, 1928: Limiting forms of the frequency distribution of the largest or smallest member of a sample. *Math. Proc. Cambridge Philos. Soc.,* **24,** 180–190.

Gnedenko, B. V., 1943: Sur la distribution limite du terme maximum d'une série aléatoire. *Ann. Math.,* **44,** 423–453.

Groisman, P. Y., R. W. Knight, D. R. Easterling, T. R. Karl, G. C. Hegerl, and V. N. Razuvaev, 2005: Trends in intense precipitation in the climate record. *J. Climate,* **18,** 1326–1350.

Gumbel, E. J., 1958: *Statistics of Extremes.* Columbia University Press, 375 pp.

Hansen, J., R. Ruedy, T. Sato, and K. Lo, 2010: Global surface temperature change. *Rev. Geophys.,* **48,** RG4004, doi:10.1029/2010RG000345.

Hardwick-Jones, R., S. Westra, and A. Sharma, 2010: Observed relationships between extreme sub-daily precipitation, surface temperature and relative humidity. *Geophys. Res. Lett.,* **37,** L22805, doi:10.1029/2010GL045081.

Hegerl, G. C., and Coauthors, 2007: Understanding and attributing climate change. *Climate Change 2007: The Physical Science Basis,* S. Solomon et al., Eds., Cambridge University Press, 663–745.

Hipel, K. W., and A. I. McLeod, 2005: *Time Series Modeling of Water Resources and Environmental Systems.* Developments in Water Science, Vol. 45, Elsevier, 1013 pp.

Jenkinson, A. F., 1955: The frequency distribution of the annual maximum (or minimum) values of meteorological elements. *Quart. J. Roy. Meteor. Soc.,* **81,** 158–171.

Kennedy, J. J., and Coauthors, 2010: How do we know the world has warmed? [in "State of the Climate in 2009"] *Bull. Amer. Meteor. Soc.,* **91** (7), S26–S27.

Kharin, V. V., and F. Zwiers, 2000: Changes in the extremes of an ensemble of transient climate simulations with a coupled atmosphere–ocean GCM. *J. Climate,* **13,** 3760–3788.

——, and ——, 2005: Estimating extremes in transient climate change simulations. *J. Climate,* **18,** 1156–1173.

——, F. W. Zwiers, X. Zhang, and G. C. Hegerl, 2007: Changes in temperature and precipitation extremes in the IPCC ensemble global coupled model simulations. *J. Climate,* **20,** 1419–1444.

——, ——, ——, and M. Wehner, 2013: Changes in temperature and precipitation extremes in the CMIP5 ensemble. *Climatic Change,* doi:10.1007/s10584-013-0705-8, in press.

Kiktev, D., D. Sexton, L. V. Alexander, and C. K. Folland, 2003: Comparison of modelled and observed trends in indicators of daily climate extremes. *J. Climate,* **16,** 3560–3571.

——, J. Caesar, L. V. Alexander, H. Shiogama, and M. Collier, 2007: Comparison of observed and multimodeled trends in annual extremes of temperature and precipitation. *Geophys. Res. Lett.,* **34,** L10702, doi:10.1029/2007GL029539.

Leadbetter, M. R., G. Lindgren, and H. Rootzen, 1983: *Extremes and Related Properties of Random Sequences and Processes.* Springer-Verlag, 336 pp.

Lenderink, G., and E. van Meijgaard, 2008: Increase in hourly precipitation extremes beyond expectations from temperature changes. *Nat. Geosci.,* **1,** 511–514.

McLeod, A. I., 2011: Kendall: Kendall rank correlation and Mann–Kendall trend test, version 2.2. R package. [Available online at http://CRAN.R-project.org/package=Kendall.]

Mears, C., B. D. Santer, F. J. Wentz, K. E. Taylor, and M. Wehner, 2007: Relationship between temperature and precipitable water changes over tropical oceans. *Geophys. Res. Lett.,* **34,** L24709, doi:10.1029/2007GL031936.

Menne, M. J., I. Durre, B. G. Gleason, T. G. Houston, and R. S. Vose, 2012: An overview of the Global Historical Climatology Network-Daily database. *J. Atmos. Oceanic Technol.,* **29,** 897–910.

Min, S. K., X. Zhang, F. W. Zwiers, P. Friederichs, and A. Hense, 2009: Signal detectability in extreme precipitation changes assessed from twentieth century climate simulations. *Climate Dyn.,* **32,** 95–111.

——, ——, F. Zwiers, and G. C. Hegerl, 2011: Human contribution to more-intense precipitation extremes. *Nature,* **470,** 378–381.

Mitchell, T. D., 2003: Pattern scaling: An examination of the accuracy of the technique for describing future climates. *Climatic Change,* **60,** 217–242.

O'Gorman, P. A., and C. G. Muller, 2010: How closely do changes in surface and column water vapour follow Clausius–Clapeyron scaling in climate change simulations? *Environ. Res. Lett.,* **5,** 025207, doi:10.1088/1748-9326/5/2/025207.

Padoan, S. A., M. Ribatet, and S. A. Sisson, 2010: Likelihood-based inference for max-stable processes. *J. Amer. Stat. Assoc.,* **105,** 263–277.

Sanchez-Lugo, A., J. J. Kennedy, and P. Berrisford, 2012: Surface temperature [in ''State of the Climate in 2011'']. *Bull. Amer. Meteor. Soc.,* **93** (7), S14–S15.

Semenov, V. A., and L. Bengtsson, 2002: Secular trends in daily precipitation characteristics: Greenhouse gas simulation with a coupled AOGCM. *Climate Dyn.,* **19,** 123–140.

Seneviratne, S. I., and Coauthors, 2012: Changes in climate extremes and their impacts on the natural physical environment. *Managing the Risks of Extreme Events and Disasters to Advance Climate Change Adaptation,* C. B. Field et al., Eds., Cambridge University Press, 109–230.

Sherwood, S. C., W. Ingram, Y. Tsushima, M. Satoh, M. Roberts, P. L. Vidale, and P. A. O'Gorman, 2010a: Relative humidity changes in a warmer climate. *J. Geophys. Res.,* **115,** D09104, doi:10.1029/2009JD012585.

——, R. Roca, T. M. Weckwerth, and N. G. Andronova, 2010b: Tropospheric water vapor, convection, and climate. *Rev. Geophys.,* **48,** RG2001, doi:10.1029/2009RG000301.

Simmons, A., K. M. Willett, P. D. Jones, P. W. Thorne, and D. Dee, 2010: Low-frequency variations in surface atmospheric humidity, temperature, and precipitation: Inferences from reanalyses and monthly gridded observational datasets. *J. Geophys. Res.,* **115,** D01110, doi:10.1029/2009JD012442.

Stephenson, A. G., 2002: EVD: Extreme value distributions. *R News,* No. 2(2), R Foundation, Vienna, Austria, 31–32. [Available online at http://CRAN.R-project.org/doc/Rnews/.]

Taylor, K. E., R. J. Stouffer, and G. A. Meehl, 2012: An overview of CMIP5 and the experiment design. *Bull. Amer. Meteor. Soc.,* **93,** 485–498.

Trenberth, K. E., 2011: Changes in precipitation with climate change. *Climate Res.,* **47,** 123–138.

——, 2012: Framing the way to relate climate extremes to climate change. *Climatic Change,* **115,** 283–290.

——, A. Dai, R. M. Rasmussen, and D. B. Parsons, 2003: The changing character of precipitation. *Bull. Amer. Meteor. Soc.,* **84,** 1205–1217.

——, and Coauthors, 2007: Observations: Surface and atmospheric climate change. *Climate Change 2007: The Physical Science Basis,* S. Solomon et al., Eds., Cambridge University Press, 235–336.

Utsumi, N., S. Seto, S. Kanae, E. E. Maeda, and T. Oki, 2011: Does higher surface temperature intensify extreme precipitation? *Geophys. Res. Lett.,* **38,** L16708, doi:10.1029/2011GL048426.

von Mises, R., 1954: La distribution de la plus grande de *n* valeurs. *Probability and Statistics,* Vol. 2, *Selected Papers of Richard von Mises,* Ph. Frank et al., Eds., American Mathematical Society, 271–294.

von Storch, H., and F. W. Zwiers, 1999: *Statistical Analysis in Climate Research.* Cambridge University Press, 484 pp.

Voss, R., W. May, and E. Roeckner, 2002: Enhanced resolution modelling study on anthropogenic climate change: Changes in extremes of the hydrological cycle. *Int. J. Climatol.,* **22,** 755–777.

Westra, S., and S. A. Sisson, 2011: Detection of non-stationarity in precipitation extremes using a max-stable process model. *J. Hydrol.,* **406,** 119–128.

Wilks, D. S., 1997: Resampling hypothesis tests for autocorrelated fields. *J. Climate,* **10,** 65–82.

——, 2011: *Statistical Methods in the Atmospheric Sciences.* Elsevier, 676 pp.

Willett, K. M., N. P. Gillet, P. D. Jones, and P. W. Thorne, 2007: Attribution of observed surface humidity changes to human influence. *Nature,* **449,** 710–713.

Zhang, X., L. V. Alexander, G. C. Hegerl, P. Jones, A. M. G. Klein Tank, T. C. Peterson, B. Trewin, and F. W. Zwiers, 2011: Indices for monitoring changes in extremes based on daily temperature and precipitation data. *Wiley Interdiscip. Rev.: Climate Change,* **2,** 851–870.